View metadata, citation and similar papers at core.ac.uk
brought to you by CORE
provided by UCL Discovery

From Tetrahedral Tetraphosphonic Acids E[*p*-$C_6H_4P(O)(OH)_2$]$_4$ (E = C, Si) to Porous Cu- and Zn-MOFs with Large Surface Areas

Alexandra Schütrumpf[a], Aysun Bulut[b,c], Nele Hermer[d], Yunus Zorlu[e], Erdoğan Kirpi[f], Norbert Stock[d], A. Özgür Yazaydın[g], Gündoğ Yücesan[b*], Jens Beckmann[a*]

Abstract: This study describes the porous MOFs Cu_2H_4STPPA·2 H_2O (**1**·2 H_2O), Zn_2H_4STPPA (**2**) and Zn_2H_4MTPPA (**3**) obtained using the tetrahedral linkers tetraphenylmethane tetrakis-4-phosphonic acid (H_8MTTPA) and tetraphenylsilane tetrakis-4-phosphonic acid (H_8STPPA) under solvothermal conditions. X-ray structures reveal 3D frameworks with large assessable voids. The percentage void volumes and the specific BET surface areas of **1** (48.7%, 794 m^2/g), **2** (48.1%, 565 m^2/g) and **3** (51.3%, 927 m^2/g) predicted by molecular simulations are among the highest reported for MOFs derived from phosphonic acids.

The recent efforts in carboxylate based metal organic frameworks (MOFs) provided valuable insight in the area of designing tailor-made three dimensional porous networks.[1] The well-established inorganic building units (IBUs) in carboxylate based MOFs provided structural control.[2] The precise isoreticular expansion of known networks has provided the desired pore sizes for storage, separation, catalysis and drug delivery.[3] Although most of the known aromatic carboxylic acid ligands have been used in MOF synthesis, vast structural potential for novel carboxylate bridging ligands and their yet unexplored properties make the MOF chemistry a very attractive research area. Organophosphonate linker molecules are the most promising candidates to take the current MOF research into a different level. Metal-organophosphonates are less air sensitive and exhibit better heat resistance compared to the present carboxylate based MOFs.[4] In addition, metal-organophosphonate frameworks provide remarkable structural diversity[5] offering a wide range of potential applications including magnetism, porosity, catalysis and bone regeneration.[6] There is not yet a methodology to control the structural diversity in metal-organophosphonate solids to synthesize predictable networks. Unfortunately, the current literature on aromatic organophosphonates and the number of known aromatic organophosphonate linkers are very limited to derive reasonable pathways towards the designed synthesis of metal organophosphonates.[4] Only few examples of isoreticular expansions of porous metal-organophosphonates have been reported, which have enabled a nitrogen donor ligand to maintain the position of the metal atoms.[7] Another method used the organoimine chelators to engineer the metal coordination to limit the number of phosphonate coordination on the metal atom.[6b] The known metal complexes of aromatic organodiphosphonates usually exhibit compact pillared-layered structures and they would exhibit tendency to pack at high densities.[4,8] One of the few reported porous metal-organophosphonate framework was synthesized using a tetrahedral tetraphosphonic acid based on a tetrahedral adamantane core.[9] Therefore the judicious choice of the bridging ligand is very important in the synthesis of porous metal organophosphonates. In this sense, tetrahedral tetraphosphonic acid ligands exhibit remarkable geometrical orientation with four open trigonal pyramidal cavities.[9,10]

In this work the recently introduced tetrahedral linkers tetraphenylmethane tetrakis-4-phosphonic acid (H_8MTTPA) and tetraphenylsilane tetrakis-4-phosphonic acid (H_8STPPA),[11] are exploited for the construction of porous metal organic frameworks with copper and zinc under solvothermal conditions (Scheme 1). Thus, the reactions of H_8STPPA with $Cu(NO_3)_2$·3 H_2O and NaOH (approx. molar ratio 1:1:2) in H_2O/MeOH (approx. volume ratio 1:1) and H_8STPPA with $ZnNO_3$ (approx. molar ratio 1:1) in H_2O/MeOH (approx. volume ratio 4:1) at 150°C provided crops of single crystals of the composition $Cu_2SiC_{24}H_{16}P_4O_8(OH)_4$·2 H_2O = Cu_2H_4STPPA·2 H_2O (**1**·2 H_2O) and $Zn_2SiC_{24}H_{16}P_4O_8(OH)_4$ = Zn_2H_4STPPA (**2**), respectively (the reaction conditions were optimized using high-throughput methods).[12] H_8MTTPA and $ZnSO_4$·7 H_2O (approx. molar ratio 1:2) was stirred briefly in dimethylformamide and heated to 180 ºC for 24 h in a PTFE-lined stainless steel acid digestion bomb, which afforded single crystals of the composition $Zn_2C_{25}H_{16}P_4O_8(OH)_4$ = Zn_2H_4MTPPA (**3**).

The crystal structure of **1**·2 H_2O shows three distinct phosphonate protonation modes, which consist of a full deprotonated RPO_3^{2-}, a half deprotonated RPO_3H^- and two fully protonated phosphonate groups RPO_3H_2 (Figure 1).

[a] Dr. A. Schütrumpf, Prof. Dr. J. Beckmann
Institut für Anorganische Chemie und Kristallographie
Universität Bremen
Leobener Straße, 28359 Bremen, Germany
*E-mail: j.beckmann@uni-bremen.de
[b] Prof. Dr. G. Yücesan
Department of Food Chemistry and Toxicology,
Technische Universität Berlin
Gustav-Meyer-Allee 25, 13355 Berlin, Germany
*E-mail: yucesan@tu-berlin.de
[c] Dr. A. Bulut
Department of Chemistry
Bogazici University
34342 Istanbul, Turkey
[d] Dr. N. Hermer, Prof. Dr. N. Stock
Institut für Anorganische Chemie
Christian-Albrechts-Universität zu Kiel
Max-Eyth-Straße 2, 24118 Kiel, Germany
[e] Prof. Dr. Y. Zorlu
Department of Chemistry
Gebze Technical University
P.O. Box 141 Gebze, 41400 Kocaeli, Turkey
[f] Dr. E. Kirpi
Department of Chemistry
Yildiz Technical University
Davutpasa Campus, Esenler, 34010 Istanbul, Turkey
[g] Dr. A. Ö. Yazaydın
Department of Chemical Engineering
University College London
London WC1E 7JE, United Kingdom
Supporting information for this article is given via a link at the end of the document.

WILEY-VCH

$H_8STPPA + Cu(NO_3)_2 + NaOH \xrightarrow{H_2O/MeOH} Cu_2H_4STPPA{\cdot}2\,H_2O$ **1**·2 H_2O

$H_8STPPA + Zn(NO_3)_2 \xrightarrow{H_2O/MeOH} Zn_2H_4STPPA$ **2**

$H_8MTPPA + Zn(NO_3)_2 \xrightarrow{DMF} Zn_2H_4MTPPA$ **3**

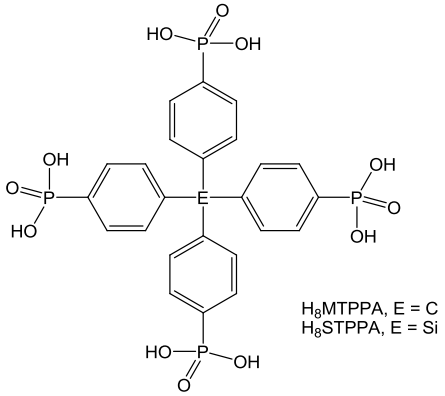

Scheme 1. Synthesis of the MOFs **1** - **3**.

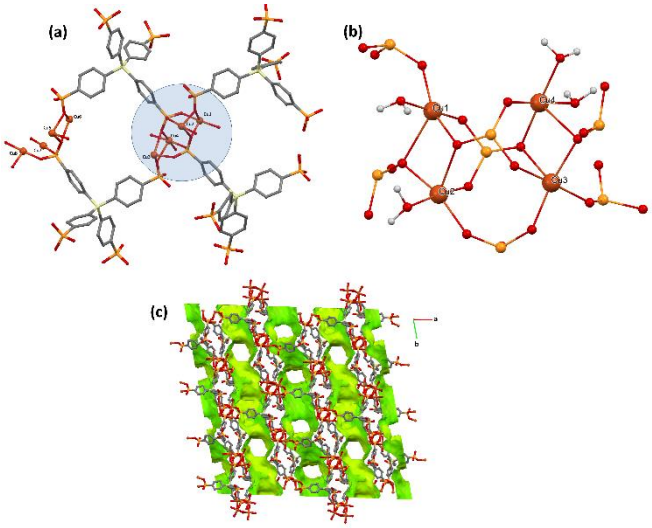

Figure 1. (a) Cu(II) coordination environment in $Cu_2H_4STPPA{\cdot}2\,H_2O$ (**1**·2 H_2O). (b) $Cu_4P_7O_{21}{\cdot}4\,H_2O$ cluster observed in **1** (c) Perspective view of three-dimensional porous framework of Cu_2H_4-STPPA ·2 H_2O (**1**·2 H_2O) along the c axis.

These phosphonate groups coordinate to the square pyramidal Cu^{2+}, two square pyramidal hydrated $\{Cu(H_2O)\}^{2+}$ and one double hydrated $\{Cu(H_2O)_2\}^{2+}$ forming the $Cu_4P_7O_{25}$ cluster (Figure 1b), which is connecting the two STPPA moieties to form the three dimensional porous framework of **1**·2 H_2O (Figure 1c). Within the tetranuclear cluster {Cu1-Cu2} and {Cu3-Cu4} show edge-sharing contact to adjacent Cu atoms to produce two distinct $\{Cu_2O_2\}$ rhombi with alternating short-long Cu-O distances. Each of the $\{Cu_2O_2\}$ rhombi are connected by two fully deprotonated and one of the half deprotonated phosphonate groups to form the cluster structure. The overall three dimensional porous framework structure of **2** and **3** is formed by connecting the 1D chain of corner-shared $Zn_2P_2O_4$ rings with H_4STPPA^{4-} and H_4MTPPA^{4-} moieties, respectively (Figures 2 and 3).

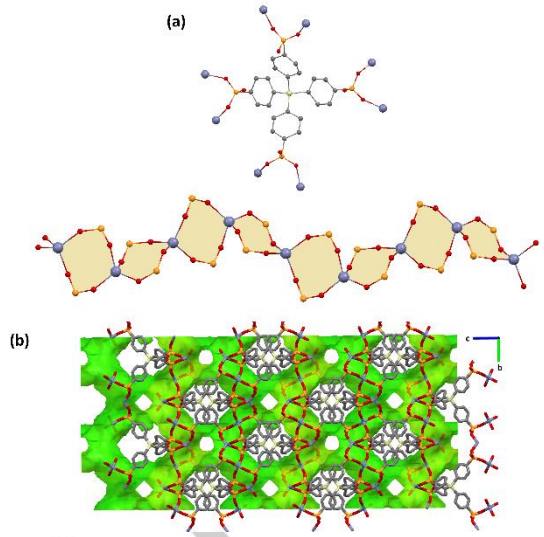

Figure 2. (a) The chain structure of corner shared $Zn_2P_2O_4$ (b) Representation of channels formed by void space within the framework of Zn_2H_4-STPPA (**2**), showing the porosity of the crystal along the a axis.

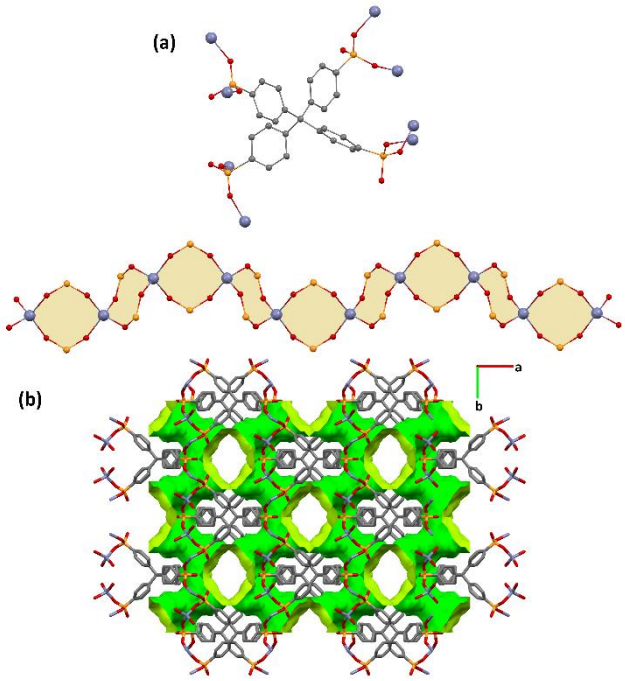

Figure 3. (a) The chain structure of corner shared $Zn_2P_2O_4$ **(b)** Perspective view of three-dimensional porous framework of Zn_2H_4-MTPPA (**3**) along ab plane.

The major difference between the structures of **2** and **3** originates as a result of angular difference between the Si and C cores in **2** and **3**, which strains the chain structure of corner-shared $Zn_2P_2O_4$ in **2** as seen in Figures 2a and 3a. Although both compounds have the same structural components and tetrahedral Zn coordination pattern, they show different porosities due to this angular difference between the Si and C cores of STPPA and MTPPA units.

Pore volumes, pore size distributions and Brunauer–Emmett–Teller (BET) surface areas of **1** - **3** were predicted with molecular simulations (Table 1 and Figure S1, see Supporting Information).

Table 1. Porosity and specific surface area of **1** - **3** predicted by molecular simulations.

	Void volume[a]	Accessible pore volume[b]	BET surface area[c]
1	48.7 %	40.0 %	794 m^2g^{-1}
2	48.1 %	33.8 %	565 m^2g^{-1}
3	51.3 %	46.0 %	927 m^2g^{-1}

[a]Computed by using a 0 Å probe size. [b]Computed by using a Helium probe. [c]Calculated by Monte Carlo simulation.

The void volumes were calculated by trial insertions of a 0 Å probe size (a randomly chosen point in the system) within the entire volume of the unit cell. This allowed us to determine the volume of the simulation cell that is not occupied by framework atoms. The accessible pore volumes were computed with the Widom insertion method[13] using a helium probe. This mimics the experimental helium porosimetry at room temperature and low pressure.[14] It should be noted that calculation of the void space is based solely on the system geometry, i.e. radii of atoms, whereas the accessible pore volume is based on a thermodynamic definition. Pore size distributions were obtained by the method of Gelb and Gubbins,[15] which is based on the largest sphere that can fit in a pore. BET surface areas were derived from N_2 adsorption isotherms at 77K which were obtained by Monte Carlo simulations in the grand canonical ensemble.[16] The percentage void volumes of all three materials are very close to each other. On the other hand, their accessible pore volumes are quite different. This is due to the presence of voids which are not accessible to guest molecules as can be clearly seen in the pore size distributions calculated for **1-3 (**Figure S1). Pores with diameters less than about 3 Å are not expected to be accessible to guest molecules. In particular, almost one third of the void volume in **2** is not accessible (48.1% vs 33.8%). Consequently, the accessible pore volume of the unit cells increases in the order **2** (33.8 %) < **1** (40.0 %) < **3** (46.0 %). Similarly, BET surface areas increase in the order **2** (565 m^2g^{-1}) < **1** (794 m^2g^{-1}) < **3** (927 m^2g^{-1}).

In summary, we report 3D porous copper and zinc organophosphonates, which were constructed using aromatic tetraphosphonic acids H_8STPPA and H_8MTPPA. Surface areas derived from Monte Carlo simulations have shown that tetrahedral aromatic organophosphonates determine the porous three-dimensional metal organic solids having exceptionally large surface areas. The Zn-MOFs **2** and **3** comprise very similar structures consisting of chains of corner-shared $Zn_2P_2O_4$ rings. The flexibility of the chains observed in **2** and **3** strengthen the hypothesis that isoreticular expansions could be possible by increasing the tether length of the tetrahedral ligands. We are currently working on producing larger surface areas following up this hypothesis.

Supporting Information Summary

X-ray crystallography, Molecular simulation, Void volumes, Accessible pore volumes, Pore size distribution, N_2-adsoption isotherms and BET surface areas. Additional references.

Acknowledgements

The Deutsche Forschungsgemeinschaft (DFG) and TÜBİTAK grant 212T060 are kindly acknowledged for financial support.

Keywords: Ligand Design • Metal Organic Solids • MOF • Organophosphonates •

References

[1] H.-C. Zhou, J. R. Long, O. M. Yaghi, *Chem. Rev.* **2012**, *112*, 673-674.

[2] a) O. M. Yaghi, M. O'Keeffe, N. W. Ockwig, H. K. Chae, M. Eddaoudi, J. Kim, *Nature* **2003**, *423*, 705-714; b) D. J. Tranchemontagne, Z. Ni, M. O'Keeffe, O. M. Yaghi, *Angew. Chem. Int. Ed*. **2008**, *47(28),* 5136-5147; c) V. Guillerm, D. Kim, J. F. Eubank, R. Luebke, X. Liu, K. Adil, M. S. Lah, M. Eddaoudi, *Chem. Soc. Rev.* **2014**, *43*, 6141-6172 and references therein.

[3] a) J. Václavík, M. Servalli, C. Lothschütz, J. Szlachetko, M. Ranocchiari, J.A. van Bokhoven, *ChemCatChem*, **2013**, *5*, 692-696; b) P. Horcajada , R. Gref , T. Baati , P. K. Allan , G. Maurin , P. Couvreur, G. Férey , R. E. Morris , C. Serre, *Chem. Rev.* **2012**, *112*, 1232-1268; c) *Nat. Mater.* **2010,** *9*, 172-178; d) G. Férey, C. Serre, T. Devic, G. Maurin, H. Jobic, P. L. Llewellyn, G. de Weireld, A. Vimont, M. Daturi, J. S. Chang, *Chem. Soc. Rev.* **2011**, *40*, 550-562; e) M. O'Keeffe and O. M. Yaghi, *Chem. Rev,*. **2012**, *112*, 675-702

[4] a) K. J. Gagnon, H. P. Perry, A. Clearfield, *Chem. Rev.* **2012**, *112*, 1034-1054; b) *Tailored Organic-Inorganic Materials*, (Eds.: E. Brunet, J. L. Colón, A. Clearfield), Wiley, **2015**.

[5] K. D. Demadis, N. Stavgianudaki, in *Metal Phosphonate Chemistry: From Synthesis to Applications*, (Eds.: A. Clearfield, K. Demadis), RSC Publishing, **2011**, pp. 438-492.

[6] a) A. Bulut, Y. Zorlu, R. Topkaya, B. Aktaş, S. Doğan, H. Kurt, G. Yücesan, *Dalton Trans.* **2015**, *44*, 12526-12529; b) A. Bulut, Y. Zorlu, E. Kirpi, A. Çetinkaya, M. Wörle, J. Beckmann, G. Yücesan, *Cryst. Growth Des.*, **2015**, *15,* 5665-5669; d) N. Hugot, M. Roger, J.-M. Rueff, J. Cardin, O. Perez, V. Caignaert, B. Raveau, G. Rogez, P.-A. Jaffrès, *Eur. J. Inorg. Chem.*, **2016**, *2016*, 266-271; e) F.-N. Shi, J. C. Almeida, L. A. Helguero, M. H. V. Fernandes, J. C. Knowles, J. Rocha, *Inorg. Chem.*, **2015**, *54(20)*, 9929-9935; f) Jean-Michel Rueff, Garyb B. Hix, Paul-Alain Jafrés, in *Tailored Organic-Inorganic Materials*, (Eds.: E. Brunet, J. L. Colón, A. Clearfield), Wiley, **2015,** pp. 376-382.

[7] a) J. A. Groves, S. R. Miller, S. J. Warrender, C. Mellot-Draznieks, P. Lightfoot, P. A. Wright, *Chem. Commun.* **2006**, 3305-3307; b) M. T. Wharmby, J. P. S. Mowat, S. P. Thompson, P. A. Wright, *J. Am. Chem. Soc.* **2011**, *133*, 1266- 1269; c) M. Taddei, F. Costantino, A. Ienco, A. Comotti, P. V Dau, S. M. Cohen, *Chem. Commun.* **2013**, *49*, 1315-1317.

[8] a) D. M. Poojary, B. Zhang, P. Bellinghausen, A. Clearfield, *Inorg. Chem.* **1996**, *35*, 5254-5263; b) B. Zhang, D. M. Poojary, A. Clearfield, *Inorg. Chem.* **1998**, *37*, 1844-1852; c) X.-M. Zhao, K.-R. Ma, Y. Zhang, X.-J. Yang, M.-H. Cong, *Inorg. Chim. Acta* **2012**, *388*, 33-36.

[9] (a) J. M. Taylor, A. H. Mahmoudkhani, G. K. H. Shimizu, *Angew. Chem.* **2007**, *119*, 809-812. (b) O. Perez, C. Bloyet, J.-M. Rueff, N. Barrier, V. Caignaert, P.-A. Jaffrès, B. Raveau *Cryst. Gowth Des*. **2016**, *16*, 6781-6789.

[10] a) Y.-B. Zhang, J. Su, H. Furukawa, Y. Yun, F. Gándara, A. Duong, X. Zou, O. M Yaghi, *J. Am. Chem. Soc.* **2013**, *135*, 16336-16339; b) M. Dinca, A. Dailly, J. R. Long, *Chem. Eur. J.* **2008**, *14*, 10280-10285

[11] a) J. K. Zareba, M. J. Bialek, J. Janczak, J. Zoń, A. Dobosz, *Cryst. Growth Des.* **2014**, *14*, 6143-6153; b) A. Schütrumpf, E. Kirpi, A. Bulut, F. L. Morel, M. Ranocchiari, E. Lork, Y. Zorlu, S. Grabowsky, G. Yücesan, J. Beckmann, *Cryst. Growth Des.* **2015**, *15*, 4925-4931.

[12] a) The high-throughput experiments were carried out as previously described: S. Bauer, C. Serre, T. Devic, P. Horcajada, J. Marrot, G. Ferey, N. Stock *Inorg. Chem.* **2008**, *47*, 7568-7576; P. Maniam, N. Stock "High-throughput Methods for the Systematic Investigation of Metal Phosphonate Synthesis Fields" in *"Metal Phosphonate Chemistry: From Synthesis to Applications"*, Edited by A. Clearfield and

K. Demadis, RSC Publishing, London (2012); N. Stock, *Microporous Mesoporous Mater.* **2009**, *129*, 287-295. b) A micro teflon container (200 μL) was charged with a 0.07 M solution of H_8-STPPA (100 μL, 5.00 mg, 70 μmol) in methanol, a 2 M solution of $Cu(NO_3)_2 \cdot 3H_2O$ (3.8 μL, 1.36 mg, 76 μmol) in water, a 1 M solution of NaOH (15.2 μL, 608 μg, 15.2 μmol) and water (81 μL) and sealed. Under autogenous pressure, the reactor was heated within 24 h to 150°C, kept for 24 h at the same temperature before it was cooled down with 16 h to room temperature. The container was opened and single crystals of Cu_2H_4STPPA·2 H_2O (**1**·2 H_2O) suitable for X-ray crystallography were hand-selected. Crystal data for **1**·2 H_2O ($C_{24}H_{24}Cu_2O_{14}P_4Si$): M = 815.48, triclinic space group *P-1*, a = 26.882(5) Å, b = 26.885(5) Å, c = 12.264(2) Å, α = 102.70(2)°, β = 101.02(2)°, γ = 76.26(2)°, V = 8308(3) Å^3, Z = 2, ρ_{calc} = 1.304, crystal dimensions 0.05 x 0.4 x 0.5, 30440 collected and 9971 unique reflections. Final residues R_1= 0.0615, wR_2= 0.1565 (I > 2σ(I)); R_1= 0.0677, wR_2= 0.1605 (all data). GooF = 0.91, 1637 parameters. SQUEZZE information: Void 1: 1456 Å^3, 352 electrons; Void 2: 1341 Å^3, 326 electrons. c) A micro teflon container (200 μL) was charged with a 0.07 M solution of H_8STPPA (40 μL, 2.00 mg, 28 μmol) in methanol, a 2 M solution of $Zn(NO_3)_2$ (3.8 μL, 0.97 mg, 76 μmol) in water and water (156 μL) and sealed. Under autogenous pressure, the reactor was heated within 24 h to 150°C, kept for 24 h at the same temperature before it was cooled down with 16 h to room temperature. The container was opened and single crystals of Zn_2H_4STPPA (**2**) suitable for X-ray crystallography were hand-selected. Crystal data for **2** ($C_{24}H_{16}O_{12}P_4SiZn_2$): M = 779.08, orthorhombic group $I2_12_12_1$, a = 12.541(3), b = 15.024(3), c = 21.730(4), V = 4094(2), Z = 4, ρ_{calc} = 1.264, crystal dimensions 0.3 x 0.4 x 0.8, 6169 collected and 2639 unique reflections. Final residues R_1= 0.0582, wR_2= 0.1563 (I > 2σ(I)); R_1= 0.0657, wR_2= 0.1622 (all data). GooF = 1.11, 201 parameters. SQUEZZE information: Void: 1298 Å^3, 77 electrons. d) A solution of $ZnSO_4 \cdot 7H_2O$ (200 mg, 0.69 mmol), MTTPA (800 mg, 1.47 mmol) in dimethylformamide (10.0 mL, 129.7 mmol) was stirred briefly and heated to 180 ºC for 24 h in a PTFE-lined stainless still acid digestion bomb. Tiny colorless crystals Zn_2H_4MTPPA (**3**) were recovered in 15% yield. Crystal data for **3** ($C_{25}H_{20}O_{12}P_4Zn_2$): M = 767.03, monoclinic space group *C2/m*, a = 23.480(5), b = 15.510(3), c = 12.560(3), β = 113.77(3), V = 4186(2), Z = 4, ρ_{calc} = 1.217, crystal dimensions 0.05 x 0.08 x 0.1, 21254 collected and 3721 unique reflections. Final residues R_1= 0.0908, wR_2= 0.2575 (I > 2σ(I)); 0.1908, wR_2= 0.2948 (all data). GooF = 1.00, 284 parameters. SQUEZZE information: Void: 1564 Å^3, 694 electrons.

[13] B. Widom, *J. Chem. Phys.* **1963**, *39*, 2802-2812.

[14] O. Talu, A. L. Myers, *Colloids Surf. A* **2001**, *187-188*, 83-93

[15] L. Gelb, K. Gubbins, *Langmuir* **1999**, *15*, 305–308.

[16] S. Brunauer, P. H. Emmett, E. Teller, *J. Am. Chem. Soc.* **1938,** *60*, 309-319

WILEY-VCH

Entry for the Table of Contents (Please choose one layout)

Layout 1:

COMMUNICATION

The percentage void volumes and the specific BET surface areas of the MOFs Cu_2H_4STPPA (**1**, 48.7%, 794 m^2/g), Zn_2H_4STPPA (**2**, 48.1%, 565 m^2/g) and Zn_2H_4MTPPA (**3**, 51.3%, 927 m^2/g) obtained from the tetraphenylmethane tetrakis-4-phosphonic acid (H_8MTTPA) and tetraphenylsilane tetrakis-4-phosphonic acid (H_8STPPA) under solvothermal conditions are amongst the highest reported for MOFs derived from phosphonic acids

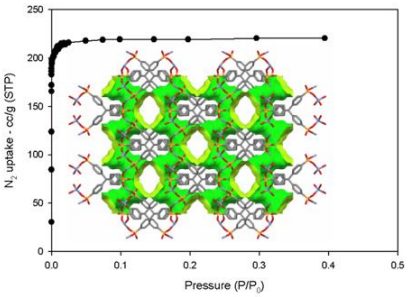

*Author(s), Corresponding Author(s)**

Page No. – Page No.

Title

WILEY-VCH